

UNCLASSIFIED

AD 410332

DEFENSE DOCUMENTATION CENTER

FOR

SCIENTIFIC AND TECHNICAL INFORMATION

CAMERON STATION, ALEXANDRIA, VIRGINIA

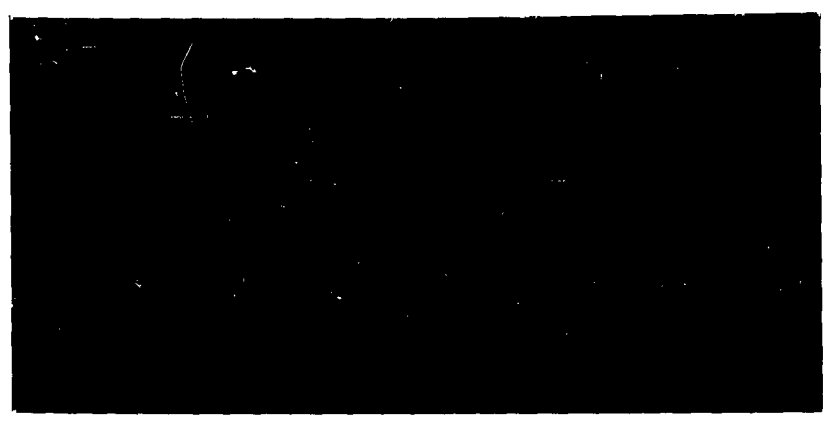


UNCLASSIFIED

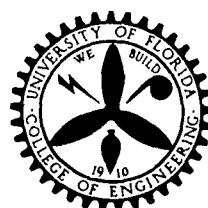
NOTICE: When government or other drawings, specifications or other data are used for any purpose other than in connection with a definitely related government procurement operation, the U. S. Government thereby incurs no responsibility, nor any obligation whatsoever; and the fact that the Government may have formulated, furnished, or in any way supplied the said drawings, specifications, or other data is not to be regarded by implication or otherwise as in any manner licensing the holder or any other person or corporation, or conveying any rights or permission to manufacture, use or sell any patented invention that may in any way be related thereto.

N-63-4-3

CATALOGED BY DDC
AS AD NO. 410332



410332



ENGINEERING AND INDUSTRIAL EXPERIMENT STATION

College of Engineering

University of Florida

Gainesville

**Best
Available
Copy**

CONTRACT NO. DA-49-186-502-ORD-860

HARRY DIAMOND LABORATORIES

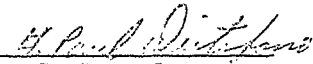
Summary Report No. 9

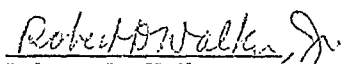
Mass Transfer In Porous Gas Diffusion Electrodes.
II. Mass Transfer Through A Single Cylindrical Pore To A
Semi-Infinite Reactive Cylinder.

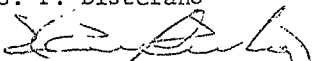
issued March 15, 1963

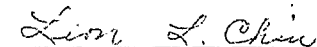
Prepared by:

Approved by:


G. P. Distefano


Robert D. Walker, Jr.


Mario Arlet


Leon L. Chiu

ENGINEERING AND INDUSTRIAL EXPERIMENT STATION

University of Florida
Gainesville, Florida

Fuel Cell Task Assignment

Contract DA-49-186-502-ORD-860
Revised Scope of Work - ORDTL-CB-762

HARRY DIAMOND LABORATORIES

Task 1 - Energy Transformation Systems

Conduct theoretical and experimental investigations to define the mechanisms and control parameters of gas diffusion electrodes in fuel cells. Work will include, but not be limited to

1. Establish a mathematical model of the overall diffusion process including terms for contributions of known mechanisms in porous media.
2. Develop expressions for contributing mechanisms which contain the physical properties of the reactants and products, and the physical properties and geometrical parameters of the electrode.
3. Conduct experimental work to verify the mathematical model.

TABLE OF CONTENTS

	<u>Page</u>
Task Assignment.....	1
1.0 SUMMARY.....	1
2.0 INTRODUCTION.....	3
3.0 MASS TRANSFER IN A POROUS ELECTRODE.....	4
3.1 Description of the Model.....	4
3.2 Flow of Oxygen in a Pore.....	4
3.3 Flow of Oxygen Through the Interface.....	5
3.4 Diffusional Transport in the Liquid.....	5
3.5 Assumptions of the Mathematical Model.....	6
3.6 Formulation of the Mathematical Model.....	8
3.6.1 Flow From Gas Phase to Gas-Liquid Interface.....	8
3.6.2 Flow From the Gas-Liquid Interface Through the Liquid.....	9
3.7 Maximum Current Density.....	17
4.0 DISCUSSION OF RESULTS.....	22
NOMENCLATURE.....	24
REFERENCES.....	27
ADDENDUM I.....	28
ADDENDUM II.....	30

1.0 SUMMARY

Previous work on mass transport limitations of porous gas diffusion electrodes (1) was extended to consider the case where the penetration of the electrolyte into a single cylindrical pore is greater than the radius of the pore so that the liquid in the pore can be considered a semi-infinite cylinder.

An elliptical concentration profile was used in this work to represent the composition in the gas-liquid interface. The major assumptions of the model are:

1. Single pore of uniform circular cross section.
2. Electrolyte penetration much greater than pore radius.
3. Instantaneous, complete, and irreversible reaction at surfaces wetted by electrolyte.
4. No reaction at dry surface.
5. Cylindrical symmetry.
6. Gas-liquid equilibrium at the interface.

The results of this work indicate that the maximum current density supportable by mass transfer is greater in the case of a semi-infinite cylinder than that deduced for a semi-infinite annulus. For an oxygen-water system this model predicts a maximum current density of 5.1 amps/cm^2 at the optimum radius of $2.15 \times 10^{-6} \text{ cm}$; for the semi-infinite annulus a maximum current density of 1.45 amps/cm^2 occurring at an optimum pore radius of $1.86 \times 10^{-6} \text{ cm}$ was found.

It was found that for a pore penetration of one pore diameter, dissolved gas reaching the pore walls wetted by the electrolyte amounted to 99.3% of the gas crossing the gas-liquid interface. This result indicates that a penetration on only one pore diameter is sufficient to make the semi-infinite cylinder the effective model.

2.0 INTRODUCTION

The model of a porous gas diffusion electrode controlled by mass transfer which was the subject of a previous report (1) has been modified to consider the case where the electrolyte penetrates an appreciable distance into the pore so that the cylinder of liquid electrolyte inside the pore can be considered semi-infinite in length.

The approach of considering the several steps involved in the total electrochemical process to be in series has been maintained. Furthermore, instantaneous and irreversible electron transfer at the reactive site, and no back diffusion of reaction products have been assumed.

The model under consideration in this investigation assumes that the inner pore walls become reactive when they are wetted by the electrolyte. Essentially all of the other assumptions of the preceeding report are considered applicable to the present model.

The principal objective of this work was to determine the conditions under which the current density resulting from the flow of oxygen through a single cylindrical pore into a semi-infinite cylinder of non-volatile electrolyte (which in other respects was assumed to act like water) was a maximum. Another objective was to determine the extent of penetration which would validate the assumption of the semi-infinite reactive cylinder.

3.0 MASS TRANSFER IN A POROUS ELECTRODE

3.1 Description of the Model

The model which was the subject of this work can be described as follows:

Pure oxygen flows through a pore of uniform circular cross-section by a combination of Poiseuille and Knudsen flows (surface flow is treated separately), followed by diffusion through a plane gas-liquid interface located in the pore due to the penetration of the electrolyte into the pore. The penetration of electrolyte into the pore is sufficiently great so that the electrolyte in the pore may be considered a semi-infinite cylinder; in principle the penetration is much greater than the radius of the pore. The reactive area is assumed to be that part of the pore wall which is wetted by the electrolyte. The oxygen diffuses from the gas-liquid interface to the pore walls where an instantaneous and irreversible electrochemical reaction occurs. It is further assumed that the reaction products do not affect the diffusion field of the dissolved oxygen.

3.2 Flow of Oxygen in a Pore

The flow of gases through a pore of small diameter may be described by three different mechanisms each of which prevails at different gas pressures.

1. Poiseuille flow is bulk flow due to a pressure gradient and occurs when the diameter of the pore is very much larger than the mean free path of the molecules of the gas.

2. Knudsen flow, occurs when the diameter of the pore is smaller than the mean free path of the molecules of the gas.

When the diameter of the pore is of a magnitude comparable to the mean free path of the gas molecules, both Poiseuille and Knudsen flows must be considered.

3. Surface flow is due to the migration of adsorbed molecules owing to a concentration gradient on the surface. The contribution to the total flow of this phenomenon is negligible for a pore diameter of the order of the mean free path of the molecules of the fluid (9) and will be neglected in the mathematical analysis of this model. However, the same type of correction as the one discussed in a previous report (1) would be applicable for the case where the surface flow could not be neglected.

3.3 Flow of Oxygen Through the Interface

Ariet and Distefano (4) cited experimental evidence in support of the thesis that the resistance of the gas-liquid interface to the diffusion of oxygen could be neglected under the flow conditions of these models. Therefore, the oxygen on the liquid side of the interface was considered to be in equilibrium with the oxygen on the gas side.

3.4 Diffusional Transport in the Liquid

The transport of the oxygen molecules from the gas-liquid interface to the reactive surface is caused by the concentration

gradient of oxygen in the liquid inside the pore. Whenever a difference in concentration of a solute exists between two points in a dilute solution there tends to be a motion of molecules of the solute from the point of high concentration to the point of low concentration. This motion can be expressed mathematically by Fick's first law

$$N_{Az} = - D_{AB} \frac{\partial C_A}{\partial z} \quad 3.4-1$$

where N_{Az} is the flux of solute A in the z direction, D_{AB} is the diffusivity (or the diffusion coefficient) of A in B, and is a measure of ability of A to move through B. It is a function of the size and shape of the molecules of solute and solvent, the temperature, and the physical state of the system. C_A is the concentration of A in the solution.

3.5 Assumptions of the Mathematical Model

The steady-state equations of motion describing the flow of oxygen from the gas phase to the reacting surface were formulated for a single cylindrical pore based on the following assumptions:

1. The distance which the electrolyte penetrates the pore is so much greater than the radius of the pore that the liquid in the pore may be considered a semi-infinite cylinder.
2. The concentration of dissolved oxygen at the interface is a function of the radius defined and discussed in a previous report (1). See page 9, B.C. III.

3. There is no reaction on the pore surface ~~not~~ wetted with electrolyte.

4. There is instantaneous, complete, and ~~and~~ irreversible reaction on the surface wetted with electrolyte.

5. The density of the gas and the diffusivity ~~activity~~ of the gas in the liquid phase as well as the viscosity of the gas are considered to be functions of temperature only.

6. In the liquid phase, the oxygen is ~~trans~~transported by diffusion only.

7. The model possesses cylindrical symmetry, i. e., no gradients in the angular direction.

8. The gas phase consists of a pure gas, ... In this investigation, the calculations are based on pure oxygen.

9. The electrolyte is non-volatile. In ~~all~~ other respects the properties of the electrolyte are assumed to be identical with those of water. This assumption obviates any counter-diffusion of electrolyte vapor in the gas phase.

10. For the mass transfer rates of this investigation, at the interface, the oxygen in the gas phase is in equilibrium with the oxygen dissolved in the liquid. The validity of this assumption has been demonstrated in an earlier report (1).

11. The flow of gas by surface migration ~~on~~ is negligible. This assumption was shown to be valid for the conditions of this model by the work of Wengrow (9).

3.6 Formulation of the Mathematical Model

3.6.1 Flow From Gas Phase to Gas-Liquid Interface

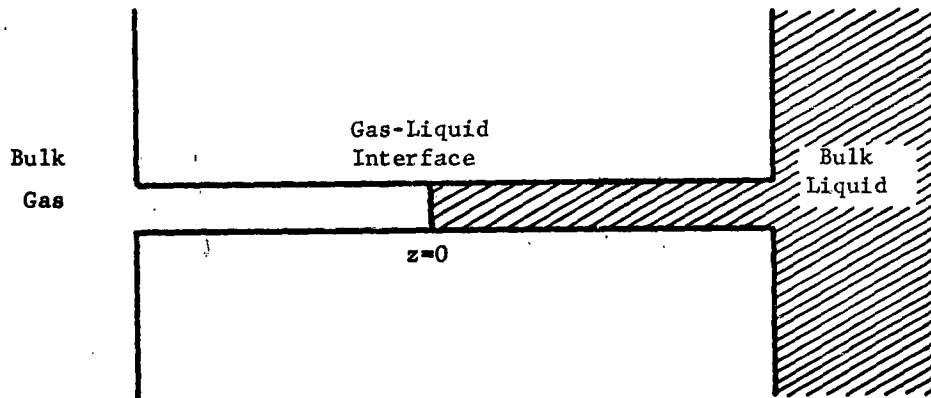


Figure 1. Schematic Diagram of Physical Model

The equation which describes the flow of oxygen from the bulk gas phase to the gas-liquid interface is the same that was developed by Ariet and Distefano (1).

$$N_{AzPG} = \frac{273}{T} \frac{(P_b - P_i)}{L} \frac{1}{22,400} \left[\frac{1.0133 \times 10^6 \times 4R^2 P}{32\eta} + \frac{4R\delta}{3} \left(\frac{2R'T}{\pi M \gamma} \right)^{\frac{1}{2}} \right] \quad 3.6-1$$

where N_{AzPG} = flux of A in the pore, in the gas phase, $\frac{\text{mol}}{\text{cm}^2\text{-sec}}$

T = absolute temperature, $^{\circ}\text{K}$

P_b, P_i = denotes pressures in the bulk gas and at the gas-liquid interface, respectively, atm.

$P = \frac{P_b + P_i}{2}$ = mean pressure, atm.

η = viscosity, poises

- R = radius of the pore, cm
 R' = ideal gas constant,
 M = molecular weight of the gas, gm.
 δ = constant defined by Carman (4)

3.6.2 Flow From the Gas-Liquid Interface Through the Liquid

Ariet and Distefano showed that the equation describing the motion of the gas from the gas-liquid interface, through the liquid, to the reactive site is Laplace's equation in cylindrical coordinates.

$$\frac{\partial^2 C_A}{\partial r^2} + \frac{1}{r} \frac{\partial C_A}{\partial r} + \frac{\partial^2 C_A}{\partial z^2} = 0 \quad 3.6-2$$

This equation is to be solved subject to the following boundary conditions which can easily be deduced from the assumptions of the model.

B.C. I At $z \geq 0$ and $r=R$, $C_A(R, z) = 0$

B.C. II At $r \geq 0$ and $z=\infty$, $C_A(r, \infty) = 0$

B.C. III At $z=0$ and $r \leq R$, $C_A(r, 0) = C_A^0 \left[1 - \left(\frac{r}{R} \right)^2 \right]^{\frac{1}{2}}$

If we apply the finite Hankel Transformation (9) to equation 3.6-2 we obtain

$$\left(\frac{d^2}{dz^2} - \alpha_j^2 \right) \bar{C}_A = 0 \quad 3.6-3$$

$$\text{where } \bar{C}_A = \int_0^R r C(r, z) J_0(\alpha_j r) dr \quad 3.6-4$$

and α_j is defined by the following equation

$$J_0(\alpha_j R) = 0 \quad 3.6-5$$

The solution of equation 3.6-3 is

$$\bar{C}_A = A e^{-\alpha_j z} + B e^{+\alpha_j z} \quad 3.6-6$$

If we apply B.C. II, then $B = 0$ and

$$\bar{C}_A = A e^{-\alpha_j z} \quad 3.6-7$$

If we apply B.C. III and the definition of the finite Hankel Transformation, we have at $z = 0$,

$$\bar{C}_A = A = \int_0^R r C_A^0 \left[1 - \left(\frac{r}{R} \right)^2 \right]^{\frac{1}{2}} J_0(\alpha_j r) dr \quad 3.6-8$$

and since this integral is independent of z , we obtain, for any value of z ,

$$\bar{C}_A = C_A^0 e^{-\alpha_j z} \int_0^R r \left(1 - \left(\frac{r}{R} \right)^2 \right)^{\frac{1}{2}} J_0(\alpha_j r) dr \quad 3.6-9$$

Now, let us consider the definition of Sonine's integral (2), where $m > n > -1$

$$J_m(x) = \frac{2x^{m-n}}{2^{m-n} \Gamma(m-n)} \int_0^1 J_n(xt) t^{n+1} (1-t^2)^{m-n-1} dt \quad 3.6-10$$

and if we let $t = \frac{r}{R}$, $dt = \frac{dr}{R}$, $\alpha_j R = x$, $n = 0$ and $m = 3/2$, then equation 3.6-10 becomes

$$J_{3/2}(\alpha_j R) = \frac{2(\alpha_j R)^{3/2}}{2^{3/2} \Gamma(3/2)} \int_0^R J_0(\alpha_j R \frac{r}{R}) \frac{r}{R} \left(1 - \left(\frac{r}{R} \right)^2 \right)^{\frac{1}{2}} \frac{dr}{R} \quad 3.6-11$$

$$J_{3/2}(\alpha_j R) = \frac{2(\alpha_j R)^{3/2}}{2^{3/2} \Gamma(3/2) R^2} \int_0^R r \left(1 - \left(\frac{r}{R} \right)^2 \right)^{\frac{1}{2}} J_0(\alpha_j r) dr \quad 3.6-12$$

If we compare the integrals in equations 3.6-9 and 3.6-12 we see that they are equal, therefore

$$\bar{C}_A = \frac{C_A^0 e^{-\alpha_j z} 2^{3/2} \Gamma(3/2) R^2}{2(\alpha_j R)^{3/2}} J_{3/2}(\alpha_j R) \quad 3.6-13$$

Now we can apply the definition of the inverse finite Hankel Transformation (9)

$$C_A = \frac{2}{R^2} \sum_{j=1}^{\infty} \frac{J_0(\alpha_j r)}{[J_1(\alpha_j R)]^2} \bar{C}_A \quad 3.6-14$$

to equation 3.6-13 we obtain

$$C_A = \frac{2}{R^2} \sum_{j=1}^{\infty} \frac{J_0(\alpha_j r)}{[J_1(\alpha_j R)]^2} \frac{C_A^0 e^{-\alpha_j z} 2^{3/2} \Gamma(3/2) R^2}{2(\alpha_j R)^{3/2}} J_{3/2}(\alpha_j R) \quad 3.6-15$$

or

$$C_A = 2^{3/2} \Gamma(3/2) C_A^0 \sum_{j=1}^{\infty} \frac{e^{-\alpha_j z}}{(\alpha_j R)^{3/2}} \frac{J_0(\alpha_j r) J_{3/2}(\alpha_j R)}{[J_1(\alpha_j R)]^2} \quad 3.6-16$$

Since (2) $\Gamma(3/2) = (\pi/4)^{1/2}$

and since (2)

$$J_{3/2}(\alpha_j R) = \left(\frac{2}{\alpha_j R \pi} \right)^{1/2} \left(\frac{\sin \alpha_j R}{\alpha_j R} - \cos(\alpha_j R) \right) \quad 3.6-17$$

then equation 3.6-16 becomes

$$C_A = 2 C_A^0 \sum_{j=1}^{\infty} \frac{e^{-\alpha_j z}}{(\alpha_j R)^2} \frac{J_0(\alpha_j r)}{[J_1(\alpha_j R)]^2} \left(\frac{\sin \alpha_j R}{\alpha_j R} - \cos \alpha_j R \right) \quad 3.6-18$$

Differentiating partially with respect to r we obtain

$$\frac{\partial C_A}{\partial r} = 2 C_A^0 \sum_{j=1}^{\infty} \frac{e^{-\alpha_j z}}{(\alpha_j R)^2} \frac{-[J_1(\alpha_j r)]}{[J_1(\alpha_j R)]^2} \alpha_j \left(\frac{\sin \alpha_j R}{\alpha_j R} - \cos \alpha_j R \right) \quad 3.6-19$$

and, if we evaluate this function at $r = R$, we obtain

$$\left. \frac{\partial C_A}{\partial r} \right|_{r=R} = 2 C_A^0 \sum_{j=1}^{\infty} \frac{e^{-\alpha_j z}}{(\alpha_j R)^2} \frac{(-\alpha_j)}{J_1(\alpha_j R)} \left(\frac{\sin \alpha_j R}{\alpha_j R} - \cos \alpha_j R \right) \quad 3.6-20$$

Since the total flow in the r direction at $r = R$ from $z = 0$ to $z = z$ is given by

$$W \Big|_{z=0}^z = \int_0^z N_{Ar} \Big|_{r=R} 2\pi R \, dz \quad 3.6-21$$

$$\text{and since } N_{Ar} \Big|_{r=R} = -D_{AB} \left. \frac{\partial C_A}{\partial r} \right|_{r=R} \quad 3.6-22$$

then

$$W \Big|_{z=0}^z = 2 C_A^0 2\pi R (-D_{AB}) \sum_{j=1}^{\infty} \frac{(-\alpha_j)}{(\alpha_j R)^2 J_1(\alpha_j R)} \left(\frac{\sin \alpha_j R}{\alpha_j R} - \cos \alpha_j R \right) \int_0^z e^{-\alpha_j z} dz \quad 3.6-23$$

$$W \Big|_{z=0}^z = 4\pi R C_A^0 D_{AB} \sum_{j=1}^{\infty} \frac{(1 - e^{-\alpha_j z})}{(\alpha_j R)^2 J_1(\alpha_j R)} \left(\frac{\sin \alpha_j R}{\alpha_j R} - \cos \alpha_j R \right) \quad 3.6-24$$

$$W \Big|_{z=0}^z = 4\pi R C_A^0 D_{AB} \sum_{j=1}^{\infty} \left[\frac{\sin \alpha_j R}{(\alpha_j R)^3 J_1(\alpha_j R)} - \frac{\cos \alpha_j R}{(\alpha_j R)^2 J_1(\alpha_j R)} \right] \left\{ \frac{1 - e^{-\alpha_j z}}{\alpha_j} \frac{\sin \alpha_j R}{J_1(\alpha_j R)} - \frac{e^{-\alpha_j z} \cos \alpha_j R}{(\alpha_j R)^2 J_1(\alpha_j R)} \right\} \quad 3.6-25$$

We can see that the last two terms of this series become zero when $z \rightarrow \infty$, which is the case when the electrolyte penetrates the pore an infinite distance. When

$$W \Big|_{z=0}^{\infty} = 4\pi R C_A^0 D_{AB} \sum_{j=1}^{\infty} \left[\frac{\sin \alpha_j R}{(\alpha_j R)^3 J_1(\alpha_j R)} - \frac{\cos \alpha_j R}{(\alpha_j R)^2 J_1(\alpha_j R)} \right] \quad 3.6-26$$

and since by equation 3.6-5, $(\alpha_j R)$ are defined to be the zeros of the Bessel function of order zero, let $\alpha_j R = x_n$, then

$$W \Big|_{z=0}^{\infty} = 4\pi R C_A^0 D_{AB} \sum_{n=1}^{\infty} \left[\frac{\sin x_n}{x_n^3 J_1(x_n)} - \frac{\cos x_n}{x_n^2 J_1(x_n)} \right] \quad 3.6-27$$

This series was evaluated in the following manner; the first ten terms were summed by an exact computation from a table of the zeros of J_0 . The terms from $n = 11$ to $n = 20$ were summed by applying the following approximations which were found to be extremely accurate for the purpose of this investigation (less than 1% error).

For $n > 10(6)$

$$J_1(x_n) = \left(\frac{2}{\pi x_n} \right)^{1/2} \cos \left(x_n - \frac{3\pi}{4} \right) \quad 3.6-28$$

and for $n > 10(5)$

$$x_n = \pi \left(n - \frac{1}{4} \right) \quad 3.6-29$$

$$\text{hence } J_1(x_n) = \left(\frac{2}{\pi \pi (n-1/4)} \right)^{1/2} \cos \left[\pi \left(n - \frac{1}{4} - \frac{3}{4} \right) \right] \quad 3.6-30$$

$$J_1(x_n) = \frac{2^{1/2} \cos \left[\pi(n-1) \right]}{\pi (n-1/4)^{1/2}} - \frac{2^{1/2} (-1)^{n-1}}{\pi (n-1/4)^{1/2}} \quad 3.6-31$$

$$\text{Now } \cos x_n = \cos \left(\pi(n-1/4) \right) = (-1)^n \cos \frac{\pi}{4} = (-1)^n \frac{2^{1/2}}{2} \quad 3.6-32$$

$$\sin x_n = \sin \left[\pi(n-1/4) \right] = (-1)^{n-1} \sin \frac{\pi}{4} = (-1)^{n-1} \frac{2^{1/2}}{2} \quad 3.6-33$$

then equation 3.6-27 becomes

$$W \Big|_{z=0}^{\infty} = 4\pi R C_A^0 D_{AB} \left\{ 0.54261 + \sum_{n=11}^{\infty} \left[\frac{(-1)^{n-1} \frac{2^{1/2}}{2} (n-1/4)^{1/2}}{\pi^3 (n-1/4)^3 \frac{2^{1/2}}{2} (-1)^{n-1}} - \frac{(-1)^n \frac{2^{1/2}}{2} (n-1/4)^{1/2}}{\pi^2 (n-1/4)^2 \frac{2^{1/2}}{2} (-1)^{n-1}} \right] \right\} \quad 3.6-34$$

$$W \Big|_{z=0}^{\infty} = 4\pi R C_A^0 D_{AB} \left\{ 0.54261 + \frac{1}{2\pi^2} \sum_{n=1}^{\infty} \left[\frac{1}{(n-1/4)^{5/2}} + \frac{\pi}{(n-1/4)^{3/2}} \right] \right\} \quad 3.6-35$$

$$W \Big|_{z=0}^{\infty} = 4\pi R C_A^0 D_{AB} \left\{ 0.54261 + \frac{1}{2\pi^2} (0.01298 + 0.56571) + \frac{1}{2\pi^2} \sum_{n=21}^{\infty} \left[\frac{1}{(n-1/4)^{5/2}} + \frac{\pi}{(n-1/4)^{3/2}} \right] \right\} \quad 3.6-36$$

$$W \Big|_{z=0}^{\infty} = 4\pi R C_A^0 D_{AB} \left\{ 0.57193 + \frac{1}{2\pi^2} \sum_{n=21}^{\infty} \left[\frac{1}{(n-1/4)^{5/2}} + \frac{\pi}{(n-1/4)^{3/2}} \right] \right\} \quad 3.6-37$$

For the determination of the infinite summation in equation 3.6-37, the Euler-Maclaurin expansion is invaluable. This expansion is given by Miller (9) as

$$\sum_{x=a}^{z-1} f(x) = \int_a^z f(\xi) d\xi + \sum_{k=a}^{m-1} \frac{B_k}{k!} \left[D^{k-1} f(z) - D^{k-1} f(a) \right] + R(m) \quad 3.6-38$$

where B_k = Bernoulli Numbers of the first kind

$$D^{k-1} f(a) = \frac{d^{k-1}}{dx^{k-1}} f(x) \Big|_{x=a}$$

$R(m) \rightarrow 0$ as $m \rightarrow \infty$

In the case of z approaching infinity, with $f(x) = \frac{1}{(x-k)^n}$, where n is positive,

$$\sum_{k=a}^{2m-1} \frac{B_k}{k!} D^{k-1} f(z)$$

is zero, and the above expansion can be written

$$\sum_{x=a}^{\infty} f(x) = \int_a^{\infty} f(\xi) d\xi - \sum_{k=1}^{\infty} \frac{B_k}{k!} D^{k-1} f(a) \quad 3.6-39$$

Therefore the first term of the infinite summation in equation 3.6-37 can be written as

$$\sum_{n=21}^{\infty} \frac{1}{(n-1/4)^{5/2}} = \int_{21}^{\infty} \frac{1}{(n-1/4)^{5/2}} dn - \sum_{k=1}^{\infty} \frac{B_k}{k!} D^{k-1} \frac{1}{(n-1/4)^{5/2}} \Big|_{n=21} \quad 3.6-40$$

The Bernoulli numbers of the first kind are given in Miller (7) as

$$B_1 = -\frac{1}{2}$$

$$B_2 = \frac{1}{6}$$

$$B_3 = B_5 = B_7 = \dots = B_{2k+1} = 0$$

$$B_4 = -\frac{1}{30}$$

$$B_6 = \frac{1}{42}$$

etc.

Equation 3.6-40 becomes

$$\begin{aligned} \sum_{n=21}^{\infty} \frac{1}{(n-1/4)^{5/2}} &= \frac{2}{3} \frac{1}{(n-1/4)^{3/2}} \Big|_{n=21} - \left[\frac{B_1}{1!} \frac{1}{(n-1/4)^{5/2}} - \frac{B_2}{2!} \frac{5}{2} \frac{1}{(n-1/4)^{7/2}} \right. \\ &\quad + \frac{B_3}{3!} \frac{5}{2} \frac{7}{2} \frac{1}{(n-1/4)^{9/2}} - \frac{B_4}{4!} \frac{5 \cdot 7 \cdot 9}{2 \cdot 2 \cdot 2} \frac{1}{(n-1/4)^{11/2}} \\ &\quad \left. + \frac{B_5}{5!} \frac{5 \cdot 7 \cdot 9 \cdot 11}{2 \cdot 2 \cdot 2 \cdot 2} \frac{1}{(n-1/4)^{13/2}} - \frac{B_6}{6!} \frac{5 \cdot 7 \cdot 9 \cdot 11 \cdot 13}{2 \cdot 2 \cdot 2 \cdot 2 \cdot 2} \frac{1}{(n-1/4)^{15/2}} \right] \Big|_{n=21} \end{aligned} \quad 3.6-41$$

The expansion on the left hand side of the equation results in an alternating series which converges very rapidly. Evaluating equation 3.6-41 at $n = 21$ results in,

$$\sum_{n=21}^{\infty} \frac{1}{(n-1/4)^{5/2}} = 0.00708 + \left[\frac{1}{2} \frac{1}{(20.75)^{5/2}} + \frac{1}{6 \cdot 2} \frac{5}{2} \frac{1}{(20.75)^{7/2}} \right. \\ \left. - \frac{1}{30 \cdot 4 \cdot 3 \cdot 2 \cdot 2 \cdot 2} \frac{5 \cdot 7 \cdot 9}{(20.75)^{11/2}} + - + - \right]$$

$$= 0.00708 + 0.000256 = 0.00734$$

3.6-42

Similarly,

$$\sum_{n=21}^{\infty} \frac{1}{(n-1/4)^{3/2}} = \int_{21}^{\infty} \frac{1}{(n-1/4)^{3/2}} dn - \sum_{k=1}^{2m-1} \frac{B_k}{k!} D^{k-1} \frac{1}{(n-1/4)^{3/2}} \Big|_{n=21} \quad 3.6-43$$

$$\sum_{n=21}^{\infty} \frac{1}{(n-1/4)^{3/2}} = 2 \frac{1}{n-1/4} \Big|_{n=21} - \left[\frac{B_1}{1} \frac{1}{(n-1/4)^{3/2}} - \frac{B_2}{2} (3/2) \frac{1}{(n-1/4)^{5/2}} \right]_{n=21} \quad 3.6-44$$

$$\sum_{n=21}^{\infty} \frac{1}{(n-1/4)^{3/2}} = 0.439 + 0.005 = 0.444 \quad 3.6-45$$

$$\pi \sum_{n=21}^{\infty} \frac{1}{(n-1/4)^{3/2}} = 1.39487 \quad 3.6-46$$

hence equation 3.6-36 becomes

$$W \Big|_{z=0}^{\infty} = 4\pi R C_A^0 D_{AB} \left[0.57193 + \frac{1}{2\pi^2} (0.00734 + 1.39487) \right] \quad 3.6-47$$

$$W \Big|_{z=0}^{\infty} = 4 R C_A^0 D_{AB} (0.64296) = 2.57 \pi R D_{AB} C_A^0 \quad 3.6-48$$

If we rewrite equation 3.6-25 as

$$W \Big|_{z=0}^z = 4\pi R C_A^0 D_{AB} \left\{ \sum_{j=1}^{\infty} \left[\frac{\sin(\alpha_j R)}{(\alpha_j R)^3 J_1(\alpha_j R)} - \frac{\cos(\alpha_j R)}{(\alpha_j R)^2 J_1(\alpha_j R)} \right] \right. \\ \left. - \sum_{j=1}^{\infty} e^{-(\alpha_j z)} \left[\frac{\sin(\alpha_j R)}{(\alpha_j R)^3 J_1(\alpha_j R)} - \frac{\cos(\alpha_j R)}{(\alpha_j R)^2 J_1(\alpha_j R)} \right] \right\} \quad 3.6-49$$

it can be seen that the total flow to the walls of the pore is equal to the flow through the gas-liquid interface only as z approaches infinity, i.e., when $e^{-\alpha_j z}$ approaches zero, the flow through the gas-liquid interface equals $W_{z=0}^{\infty}$.

Although the first summation in equation 3.6-27 converged so slowly that the application Euler-Maclaurin expansion was necessary to perform the summation, the second summation converged very rapidly because of the term $e^{-(\alpha_j z)}$. This second summation was carried out term by term, and for values of z greater than one pore radius, four terms were sufficient to represent the infinite summation.

Values of the flow that reach the pore walls were calculated for different values of z , and the results are shown in Figure 2. It can be seen that when z is equal to $2R$ (electrolyte penetration of one pore diameter) 99.3% of the flow through the interface reaches the inside of the pore wall wetted with electrolyte. This is very significant for porous gas diffusion electrodes for it means that a pore penetration by the electrolyte of one pore diameter is sufficient to make the semi-infinite cylinder the effective model.

3.7 Maximum Current Density

The flow of gas through the gas phase and through the gas-liquid interface are equal because they are in series. Since the area that flux is based on is taken to be the same, viz., the cross-sectioned area of the pore, the flux through the gas phase can be equated to

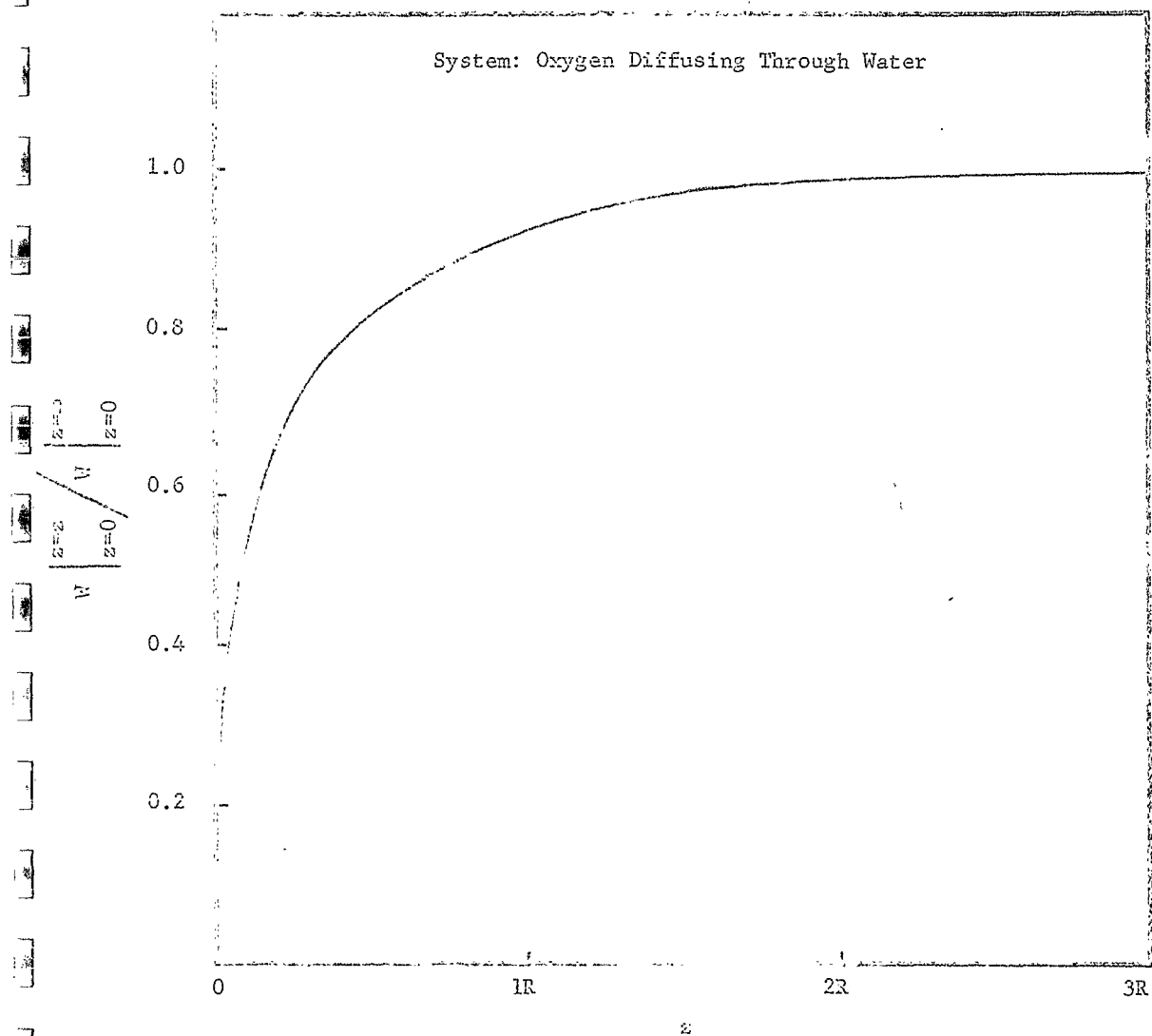


Figure 2. Fraction of Gas Flow Through Gas-Liquid Interface Reaching Pore Walls

the flux through the gas-liquid interface.

$$N_{ALPG} = N_{azi} \quad 3.7-1$$

where N_{ALPG} = Flux of oxygen through the pore in the z direction in the gas phase.

N_{azi} = flux of oxygen through the interface.

The flow of oxygen through the interface was shown to be equal to the total flow to the pore wall in an infinite distance from the interface. The flux of oxygen through the interface is therefore given by

$$N_{azi} = N_{LR} = \frac{\int_0^\infty N_{Ar} \cdot 2\pi r dr}{\int_0^\infty 2\pi r dr} = \frac{W}{\pi R^2} = 2.57 D_{AB} \frac{C_A^0}{R} \quad 3.7-2$$

where N_{LR} = total flux to the pore wall in the distance $z = \infty$.

N_{Ar} = flux in the r direction at any point r, z .

W = total flow to the pore wall in the distance $z = \infty$.

Since we can express the concentration C_A as a function of the interfacial pressure by Henry's law

$$C_A = \frac{P}{H} \quad 3.7-3$$

where P_i = pressure at the interface

H = Henry's Law constant

equation 3.7-2 becomes

$$N_{A21} = N_{AR} \quad n=0 = \frac{2.57 P_{AR} P_1}{18 R R} \quad 3.7-4$$

N_{A20} is given by equation 3.6-2 as

$$N_{A20} = \frac{273}{T} \frac{P_1 - P_2}{L} \frac{1}{22,400} \left[\frac{1.0135 \times 10^6 \times 45^2}{32 \eta} + \frac{4}{3} R \delta \left(\frac{2RT}{\pi M} \right)^{1/2} \right] \quad 3.7-5$$

To illustrate the calculation of the optimum pore diameter we use 3.7-4 and 3.7-5 in 3.7-1 under the following conditions

$$T = 300^\circ K$$

$$\eta = 2.0 \times 10^{-4} \text{ poises (g)}$$

$$L = 0.1 \text{ cm}$$

$$M = 32 \text{ g/mol}$$

$$\delta = 1.0$$

$$R' = 0.01 \times 10^7 \text{ ergs/gmol}^\circ K$$

$$D_{A1} = 1.5 \times 10^{-5} \text{ cm}^2/\text{sec (g)}$$

$$A = 1.0 \times 10^4 \text{ cm}^2 \text{ (g)}$$

$$P_1 = 1 \text{ atm}$$

Therefore equation 3.7-1 becomes

$$\frac{273}{300} \frac{(1 - P_2)}{0.1} \frac{1}{22,400} \left[\frac{1.0135 \times 10^6 \times 45^2}{32 \times 2.0 \times 10^{-4}} + \frac{4}{3} R \left(\frac{2 \times 0.01 \times 10^7 \times 300}{\pi \times 32} \right)^{1/2} \right] = \frac{2.57 \times 1.0 \times 10^4 P_2}{18 \times 1.5 \times 10^{-5} \times} \quad 3.7-6$$

Algebraic manipulation of equation 3.7-6 results in

$$5.58 \times 10^{-11} \frac{P_i}{1-P_i} = R^2 \left[1.29 \times 10^5 R (1+P_i) + 12.1 \right] \quad 3.7-7$$

Under the restriction that P_i and R be related as in equation 3.7-7, we obtain a maximum flux to the pore walls $(N_{AR})_{\max} \Big|_{z=0}^{\infty}$ at an optimum radius of 2.15×10^{-6} cm. The interfacial pressure corresponding to this radius was computed to be 0.51 atm. The maximum flux to the pore walls under these conditions is, from equation 3.7-4,

$$(N_{AR})_{\max} \Big|_{z=0}^{\infty} = 1.32 \times 10^{-5} \text{ moles/cm}^2 \cdot \text{sec.}$$

Therefore, the maximum current density which can be supported by mass transfer to a reactive site is (assuming 4 electrons per molecule of oxygen)

$$\begin{aligned} (i_m)_{\max} &= (N_{AR})_{\max} \Big|_{z=0}^{\infty} \frac{\text{mol}}{\text{cm}^2 \cdot \text{sec.}} 3.86 \times 10^5 \frac{\text{amps sec}}{\text{mol}} \\ &= 5.1 \frac{\text{amps}}{\text{cm}^2} \end{aligned}$$

4.0 DISCUSSION OF RESULTS

The value for the maximum current density predicted by this model is approximately three times greater than the value obtained by Ariet and Distefano under the assumption of no electrolyte penetration in the pore (semi-infinite annulus) (1). This higher value may be explained by the fact that the liquid phase diffusion path is shorter when the electrolyte penetrates into the pore than when the gas has to diffuse into the liquid outside the electrode to get to the annular reactive area. Furthermore, it is conventional to calculate the current density based on the geometric area of the electrode. The area considered in this case is only the cross-sectional area of the pore whereas in the case of no penetration the area is the cross-sectional area of the pore plus the annular reactive area.

One of the major assumptions of this model is that the liquid penetrates the pore to such an extent that the pore can be considered a semi-infinite cylinder. An important question immediately arises: What depth of penetration relative to the pore radius is necessary to constitute a semi-infinite cylinder? From Figure 2 it can be seen that at an electrolyte penetration of one pore radius 92.4 per cent of the flow through the gas-liquid interface reacts on the pore wall. At a penetration of only one pore diameter, 99.3 per cent of this flow reacts on the pore wall. It was concluded from these results that any penetration depth greater than one pore diameter is sufficient to constitute a semi-infinite cylinder.

The assumption that the presence of the reaction products on the reactive sites does not alter the diffusion rates of the oxygen in the liquid will produce a higher value for the current density than the true physical model in which these reaction products will probably be a serious obstacle to the diffusion of oxygen in the liquid inside the pore. It should be obvious that as the wetting proofing agent is oxidized and the liquid penetrates in a pore whose inner walls are not activated, the diffusion rate of the oxygen to get to a reactive site will be much slower because the gas will have to diffuse a longer distance in the liquid where the diffusion coefficient is much lower than in the gas phase. This will result in a decrease in the current density. This effect is commonly referred to as the "drowning" of the electrode. When the inner walls of the pore are activated, the penetration of the liquid in the pore will produce an increase in the current density according to the results of this study. This seems to indicate that it is desirable to activate the inner pore walls of porous electrodes rather than to activate only the outer surface of the electrodes.

NOMENCLATURE

A	Represents component A in the binary system of A and B
B	Represents component B in the binary system of A and B
B_k	Bernoulli numbers of the first kind of order k
C_A	Concentration of component A at any point (r,z), mol/cm. ³
\bar{C}_A	Concentration of component A at any point (r, ξ), mol/cm. ³
C_A^o	Concentration of component A at the point (0,0), mol/cm. ³
D_{AB}	Diffusivity of A through B, cm ² /sec.
H	Henry's Law constant, atm.
J_j	Bessel function of the first kind of order j
L	Length of pore not penetrated by the liquid
M	Molecular weight of the gas
n	Defined by equation 3.6-29
N_{Ar}	Molar flux of component A in the r-direction at any point (r,z), moles/cm. ² sec.
$N_{AR} _{z=0}^z$	Total molar flux of component A to the reactive pore site in the region z=0 to z=z
N_{Az}	Molar flux of component A in the z-direction at any point (r,z), moles/cm. ² sec.
N_{Azi}	Total molar flux of component A through the gas-liquid interface, mol/cm. ² sec.
N_{AzPG}	Molar flux of component A in the gas-phase area of the inside of the pore, mol/cm. ² sec.
P	Average pressure in the pore, $\frac{P_b + P_i}{2}$, atm.
P_b	Bulk gas pressure, atm
P_i	Gas-liquid interfacial pressure, atm

r	Denotes radial direction, cm
R	Radius of the pore, cm
R'	Gas constant in appropriate units
t	Denotes time, sec
T	Denotes temperature, $^{\circ}\text{K}$
$W \Big _{z=0}^z$	Total moles of flow to the pore walls in the region $z=0$ to $z=z$, moles/sec.
x_n	Defined by equation 3.6-29
z	Denotes axial direction, cm

SUBSCRIPTS

A	Denotes the component A in the binary mixture of A and B
B	Denotes the component B in the binary mixture of A and B
b	Denotes the bulk gas
G	Denotes the gas
i	Denotes the gas-liquid interface
j	Denotes the j^{th} root of the first order Bessel function of the first kind, $J_1(\alpha_j R) = 0$
k	Denotes the k^{th} order Bernoulli number of the first kind, B_k
n	Denotes the n^{th} root of the first order Bessel function of the first kind, $J_1(x_n) = 0$
P	Denotes the pore
R	Denotes the reactive pore area
r	Denotes the radial direction
z	Denotes the axial direction

GREEK SYMBOLS

δ	Constant defined by Carman (3)
η	Viscosity of the gas, poise
α_j	Defined by equation 3.6-5
ρ	partial pressure of oxygen, atm

REFERENCES

1. Ariet, M. and Distefano, G.P., Summary Report No. 8, University of Florida, March 15, 1963.
2. Bowman, Frank, "Introduction to Bessel Functions", p. Dover Publications, Inc., New York (1958).
3. Carslaw, H.S. and Jaeger, J.C., "Conduction of Heat in Solids", Oxford Press, London (1959).
4. Carman, P.C., Proc. Roy. Soc., 203 A, 55, London (1950).
5. Janke, E. and Emde, F., "Table of Functions", 4th ed., p. Dover Publications, Inc., New York (1945).
6. Mickley, H.S., Sherwood, T.K. and Reed, C.E., "Applied Mathematics in Chemical Engineering", p. 176, McGraw-Hill Book Company, New York (1957).
7. Miller, K.S., "An Introduction to the Calculus of Finite Differences and Difference Equations", p. 113, Henry Holt and Co., New York (1960).
8. Perry, J.H., "Chemical Engineer's Handbook", 3rd ed., McGraw-Hill, New York (1950).
9. Sneddon, I.N., "Fourier Transforms", p. 104, McGraw-Hill Book Co., New York (1951).
10. Wengrow, Henry, Summary Report No. 6, University of Florida, December 15, 1962.

ADDENDUM I

Computation of Concentration Profiles

Concentration profiles as a function of r/R with z/R as a parameter are shown in Figure 3. The values of C_A/C_A^0 were calculated from a truncated form of the infinite series in equation (3). This equation resulted in a convergent series containing alternating terms. In all cases, six or seven terms were sufficient to insure that the truncated series was an adequate representation of the infinite series.

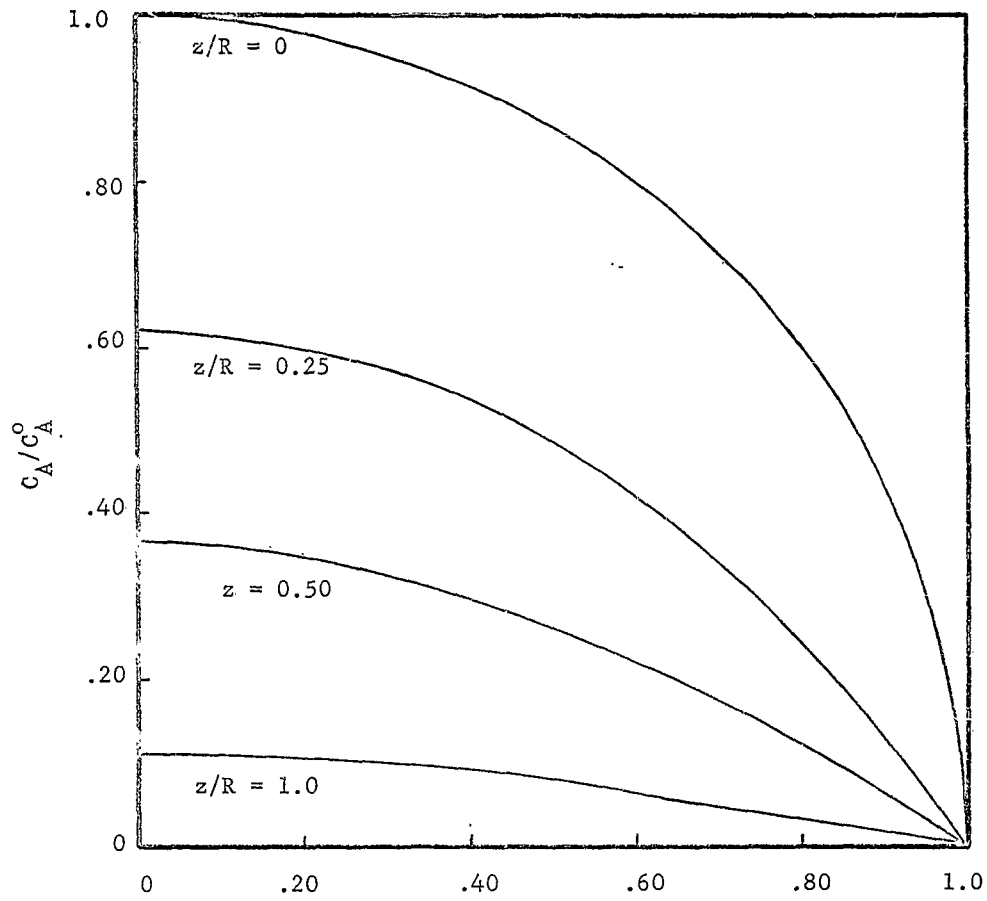


Figure 3. Plot of C_A/C_A^0 Versus r/R with z/R as a Parameter

ADDENDUM II

The System Air-Water

It was shown in a previous report* that for an air-water system, the oxygen flow through a stagnant layer of nitrogen in the pore can be calculated using the partial pressure differential of oxygen as the driving force. When the bulk gas pressure of air is $P_b = 1.0$ atm the bulk partial pressure of oxygen is approximately $p_b = 0.2$ atm. If all other conditions are identical, and the contribution of Poiseuille flow is neglected, equation 3.7-5 becomes

$$N_{AzPG} = 12.05 (0.2 - p_i) \quad (1a)$$

Equating equations 3.7-4 and (1a) results in

$$12.05 (0.2 - p_i) = 5.58 \times 10^{-11} \frac{p_i}{R} \quad (2a)$$

Under the constraint of equation (2a), the optimum pore radius is 2.15×10^{-6} cm, with a corresponding interfacial partial pressure $p_i = 0.1$ atm. Under these conditions the maximum current density obtained is 1.0 amp/cm^2 .

* Ariet, M. and Distefano, G.P., Summary Report No. 8, University of Florida, March 15, 1963.